Journal of proteome research

Article

pubs.acs.org/jpr

# Integrated Transcriptomic and Glycomic Profiling of Glioma Stem Cell Xenografts

Norelle C. Wildburger,[†,▽] Shiyue Zhou,[⊥,▽] Lauren G. Zacharias,[⊥] Roger A. Kroes,[∥] Joseph R. Moskal,[∥] Mary Schmidt,[∥] Parvin Mirzaei,[⊥] Joy Gumin,[#] Frederick F. Lang,[#] Yehia Mechref,[*,⊥] and Carol L. Nilsson[*,‡,§]

[†]Neuroscience Graduate Program, Graduate School of Biomedical Sciences, [‡]Department of Pharmacology & Toxicology, and [§]UTMB Cancer Center, University of Texas Medical Branch, 301 University Blvd, Galveston, Texas 77555-1074, United States

[⊥]Department of Chemistry and Biochemistry, Texas Tech University, 2500 Broadway, Lubbock, Texas 79409, United States

[∥]The Falk Center for Molecular Therapeutics, McCormick School of Engineering and Applied Sciences, Northwestern University, 1801 Maple Street, Evanston, Illinois 60201, United States

[#]Department of Neurosurgery and The Brain Tumor Center, The University of Texas M.D. Anderson Cancer Center, 1515 Holcombe Boulevard, Houston, Texas 77030, United States

Supporting Information

**ABSTRACT:** Bone marrow-derived human mesenchymal stem cells (BM-hMSCs) have the innate ability to migrate or home toward and engraft in tumors such as glioblastoma (GBM). Because of this unique property of BM-hMSCs, we have explored their use for cell-mediated therapeutic delivery for the advancement of GBM treatment. Extravasation, the process by which blood-borne cells—such as BM-hMSCs—enter the tissue, is a highly complex process but is heavily dependent upon glycosylation for glycan−glycan and glycan−protein adhesion between the cell and endothelium. However, in a translationally significant preclinical glioma stem cell xenograft (GSCX) model of GBM, BM-hMSCs demonstrate unequal tropism toward these tumors. We hypothesized that there may be differences in the glycan compositions between the GSCXs that elicit homing ("attractors") and those that do not ("non-attractors") that facilitate or impede the engraftment of BM-hMSCs in the tumor. In this study, glycotranscriptomic analysis revealed significant heterogeneity within the attractor phenotype and the enrichment of high mannose type *N*-glycan biosynthesis in the non-attractor phenotype. Orthogonal validation with topical PNGase F deglycosylation on the tumor regions of xenograft tissue, followed by nLC−ESI−MS, confirmed the presence of increased high mannose type *N*-glycans in the non-attractors. Additional evidence provided by our glycomic study revealed the prevalence of terminal sialic acid-containing *N*-glycans in non-attractors and terminal galactose and *N*-acetyl-glucosamine *N*-glycans in attractors. Our results provide the first evidence for differential glycomic profiles in attractor and non-attractor GSCXs and extend the scope of molecular determinates in BM-hMSC homing to glioma.

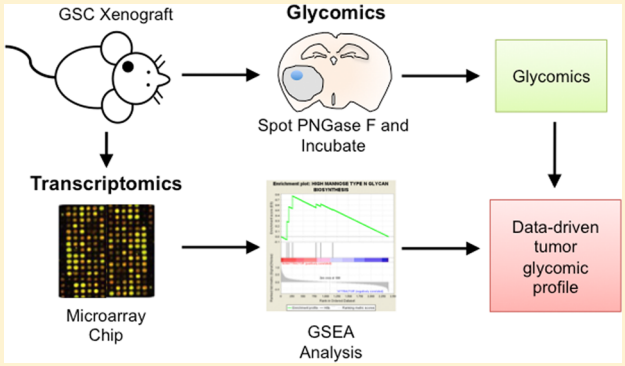


**KEYWORDS:** *glioblastoma, bone marrow-derived human mesenchymal stem cells (BM-hMSCs), transcriptomics, glycomics, N-linked glycosylation, high-mannose, sialic acid*

## INTRODUCTION

Glycosylation is the most common protein post-translational modification (PTM). It is estimated that 50% of all proteins within the human proteome are glycosylated, though only 10% of proteins have evidence supporting the presence of this PTM.[1,2] The glycan moieties on membrane and secreted proteins are important modulators of protein folding, stability, and trafficking.[2,3] Glycosylation also mediates biological functions such as cell−cell or cell−matrix adhesion,[2,4−6] host−pathogen interactions,[2,6,7] and receptor−ligand interactions.[6,8] One important cell−cell adhesion process critically reliant on and predominantly mediated by glycan moieties is extravasation.

Extravasation is the process whereby cells within blood vessels home or migrate to sites of inflammation or damaged tissue.[5,9] In the first step, rolling adhesion, carbohydrate−carbohydrate interactions are critical.[9,10] Carbohydrate binding proteins (e.g., P- and E-selectin) on the endothelial surface recognize and bind carbohydrates (e.g., Sialyl Lewis$^X$) on glycolipids or glycoproteins on the opposing cell surface. The

**Received:** May 5, 2015
**Published:** July 17, 2015





DOI: 10.1021/acs.jproteome.5b00549
*J. Proteome Res.* 2015, 14, 3932−3939

next step, tight binding, predominantly relies on complementary pairs of adhesion molecules on the opposing cell surfaces to strengthen the initial interaction established by rolling adhesion. Many adhesion proteins, such as integrins and ICAMs, are themselves heavily glycosylated.[9,10] The importance of glycosylation in extravasation is highlighted by the consequences of genetic deletion of enzymes related to *O*- and *N*-linked glycan processing.[10] For instance, mice lacking polypeptide *N*-acetylgalactosamine transferase-1 (*Galnt1*$^{-/-}$), which initiates *O*-linked glycosylation, demonstrate significantly reduced extravasation at every critical step.[11] Genetic ablation of sialyltransferase ST3Gal-IV in mice reduced CXCR2-mediated firm adhesion.[12]

Recent observations of intra-arterially delivered bone marrow-derived human mesenchymal stem cells (BM-hMSCs), for cell-based therapeutic delivery of antiglioma agents,[13−19] suggest that these cells extravasate from the blood vessel endothelium via diapedesis after intravascular injection to engraft into the tumor mass.[15] GFP-labeled BM-hMSCs injected into the internal carotid artery of tumor-bearing mice were found in linear arrangements co-localized with endothelial marker CD31 up to two days post-treatment.[15] By the third day, BM-hMSCs were seen dispersed throughout the tumor parenchyma, supporting the hypothesis of extravasation-mediated localization.[15] However, the fact that some GSCXs attract BM-hMSCs ("attractors") and others do not ("non-attractors") suggests that there are differences in the tumor-expressed glycans,[14] which may make attractors conducive to BM-hMSC engraftment.

We have previously found alterations in the lipid compositions[20] and proteins comprising cell-signaling pathways[21] of the attractor and non-attractor GSCXs, which have shed light on the different phenotypes. We have analyzed the glycomic profiles of U373MG xenografts[22] and glioma stem cells,[23] but the differential glycan profiles of attractor and non-attractor GSCXs remains unexamined. Thus, we set out to evaluate the glycan profiles of these tumors to expand our understanding of the variable BM-hMSC tropism. We first used glycogene-targeted transcriptomics to generate an informed data-driven glycomics approach. Data derived from targeted glyco-microarrays prompted an *N*-linked glycan-specific approach using on-tissue digestion of *N*-glycans from the tumor areas of attractor and non-attractor xenografts followed by nLC−ESI−MS analysis.[24]

## MATERIALS AND METHODS

### Chemicals and Reagents

Borane−ammonia complex, sodium hydroxide beads, dimethyl sulfoxide (DMSO), iodomethane, trifluoroacetic acid, chloroform, ammonium bicarbonate, and MS-grade formic acid were obtained from Sigma-Aldrich (St. Louis, MO). Microspin columns were supplied by Harvard Apparatus (Holliston, MA). PNGase F (500,000 units/mL) was purchased from New England Biolabs Inc. (Ipswich, MA). Acetic acid and acetonitrile were purchased from Fisher Scientific (Pittsburgh, PA), and HPLC-grade water was acquired from Mallinckrodt Chemicals (Phillipsburg, NJ).

### Animals

Male athymic nude mice (*nu/nu*) were purchased from the Department of Experimental Radiation Oncology, The University of Texas M.D. Anderson Cancer Center (MDACC, Houston, TX) as previously described.[20,21] All animal procedures were undertaken within the guidelines prescribed by the MDACC Animal Care and Use Committee, the USDA Animal Welfare Act, and the Guide for the Care and Use of Laboratory Animals (NIH).

### Glioma Xenograft Model

GSCs (GSC17, GSC11, GSC229, GSC231, GSC268, and GSC274) were established as previously described.[25,26] GSCs ($1 \times 10^6$) were implanted in mice via the guide-screw method.[27] Nine attractors (GSCX17, GSCX268, and GSCX274) from three different cell lines each with three biological replicates, and nine non-attractors (GSCX11, GSCX229, and GSCX231) from three different cell lines each with three biological replicates were used for this study. A total of 18 GSCXs, nine biological replicates per phenotype, were used in this study. Attractor and non-attractor phenotypes were determined previously.[14]

### Tissue Dissection, Sectioning, and Sampling

Animals were anesthetized by intraperitoneal injection of ketamine/xylazine and sacrificed as previously described.[20] Brains were removed immediately, flash frozen in liquid nitrogen vapor,[28] and sliced to 1.5-mm thick using a brain matrix. Tissue punches (1.5 mm diameter; Braintree Scientific, Braintree, MA) were taken from the tumor site within each slice and flash frozen in liquid nitrogen as previously described.[21] Next, brain tissue was sectioned at 20 $\mu$m along the coronal plane and thaw mounted on glass slides for on-tissue deglycosylation.[24] Slides were stored at −80 °C until further analysis.

### Targeted Transcriptomic Analysis

Transcriptomic experiments were conducted on a custom targeted microarray chip containing functional human gene sets related to glioma biology compiled from the NCBI human sequence database as previously described.[21,29−31] Briefly, total RNA was extracted from all individual biological replicates of GSCXs ($N$ = 9 attractors; $N$ = 9 non-attractors), purified, amplified, and then labeled with Cy5. A universal human reference (Stratagene, La Jolla, CA) was labeled with Cy3.[32] Data from chips scanned with a confocal laser (ScanArray 4000XL; Packard Biochip Technologies, Billerica, MA) were processed with BlueFuse (Illumina Fulbourn, Cambridge, UK)[21,29−31] and analyzed by significance of analysis of microarrays algorithm (SAM, v4.0, Stanford University, Palo Alto, CA).[33] The significance cutoff was set to an FDR of <10%.[21,29−31] As previously described,[21] positive fold change values are indicative of an increase in transcript expression in attractors relative to non-attractors, and negative fold change values are indicative of a decrease in transcript expression in attractors relative to non-attractors (Supplemental Table 1, Supporting Information). This data set[21] was re-analyzed by Gene Set Enrichment Analysis (GSEA) to determine significantly enriched glycomic pathways from a custom-made glycomic pathway database.[34−36] Significantly enriched data sets are defined at $p < 0.05$ and a false discovery rate (FDR) of $q < 0.30$. DanteR (version 0.1.1) was used to generate a 3D PCA of all glycogenes from GSCXs.

### On-tissue Digestion

Coronal sections (20 $\mu$m) of all GSCXs were brought to room temperature and spotted with 1 $\mu$L of PNGase F (50 Units) on the tumor regions of attractor and non-attractor xenografts. The enzymatic deglycosylation reaction was carried out overnight in a water bath at 37 °C. Released *N*-glycans were



DOI: 10.1021/acs.jproteome.5b00549
J. Proteome Res. 2015, 14, 3932−3939

collected and reduced with borane−ammonia, followed by solid-phase permethylation (SPP) as previously described.[24]

### NanoLiquid Chromatography−Mass Spectrometry

Samples resuspended in 20% acetonitrile/0.1% FA were subjected to nanoLC−MS analysis as previously described[24,37−40] in a Dionex Ultimate 3000 UHPLC system (Thermo Scientific, Sunnyvale, CA, USA) coupled to an LTQ Orbitrap Velos (Thermo Scientific, San Jose, CA, USA) mass spectrometer. The flow rate of the nanoLC system was set to 350 nL/min. Mobile phase A consisted of 98% water, 2% acetonitrile, and 0.1% formic acid, whereas mobile phase B consisted of 100% acetonitrile and 0.1% formic acid. Permethylated glycans were separated on a $C_{18}$ column (Thermo Scientific, Pittsburgh, PA, USA) using these conditions: 20% mobile phase B for 10 min, 20−38% B in 1 min, 38−60% B over 35 min, and finally, 90% B was applied and held for 5 min. The column oven temperature was set to 55 °C. The nanoLC system was coupled to the mass spectrometer using a nanoelectrospray ionization source. The resolution of full MS was set to 15,000, which is adequate to resolve close glycan $m/z$ values. MS/MS was conducted in data-dependent acquisition (DDA) mode; the four most intense peaks were subjected to MS/MS analysis using both collision-induced dissociation (CID) and higher-energy collisional dissociation (HCD).

## DATA PROCESSING AND ANALYSIS

MultiGlycan[41,42] was employed to process the raw data files generated by the mass spectrometer. First monoisotopic peaks within 6 ppm difference from theoretical $m/z$ values and with correct charge states were extracted. The theoretical $m/z$ values were generated from a comprehensive *N*-glycan candidate list consisting of 128 glycans with different charge states and adduct forms (e.g., protonated, sodiated, and ammoniated). The peak areas of extracted ion chromatograms were used to represent the abundance of each glycan structure detected in the different samples. The same glycan structures across consecutive MS scans were merged,[42] and each injection was normalized according to the digestion area on tissue slides. Data were filtered based on percent missing values (%NA) with >50% NA removed. Grubb's test was used to identify and remove outliers in the data set. Data presented as mean ± SEM with $p \leq 0.05$ considered significant.

## RESULTS

The glycomics of GSCXs exhibiting differential homing for attractors and non-attractor BM-hMSCs have not been systematically studied. Because glycans are essential to the extravasation process,[2,10] it is critical to gain a better understanding of the differential glycan profiles of the attractor and non-attractor phenotypes. We employed the workflow outlined in Figure 1 to investigate glycotranscripts and *N*-glycans differentially expressed in GSCXs exhibiting attractor and non-attractor phenotypes.

## TARGETED TRANSCRIPTOMICS REVEALS ENRICHMENT OF HIGH MANNOSE TYPE *N*-GLYCANS IN NON-ATTRACTOR PHENOTYPE

Our previously published data from these same GSCXs using a targeted microarray platform containing 2,577 total transcripts related to glioma biology was re-analyzed, focusing on all the cloned human glycogenes contained on the chip[21] (Supplemental Table 1, Supporting Information). PCA analysis of all glycotranscripts from attractors and non-attractors (Figure 2A) demonstrated clear separation between the two phenotypes (PC1). The clustering of biological replicates (individual animals with the same cells line) for attractors (PC3, 8.13%) and non-attractors (PC2, 9%) was similar. However, from the overall clustering of both individual cells lines (e.g., GSC17) and biological replicates within a given phenotype, the attractors demonstrated greater glycotranscript heterogeneity compared to non-attractors. GSEA analysis of the transcripts using a custom-made glycogene database revealed high mannose type *N*-glycan biosynthesis (nominal $p$-value = 0.0383; FDR $q$-value = 0.2962) to be significantly enriched in the non-attractor phenotype (Figure 2B). However, no glycan synthesis or degradation pathway met our threshold requirements in GSEA for attractors (data not shown).

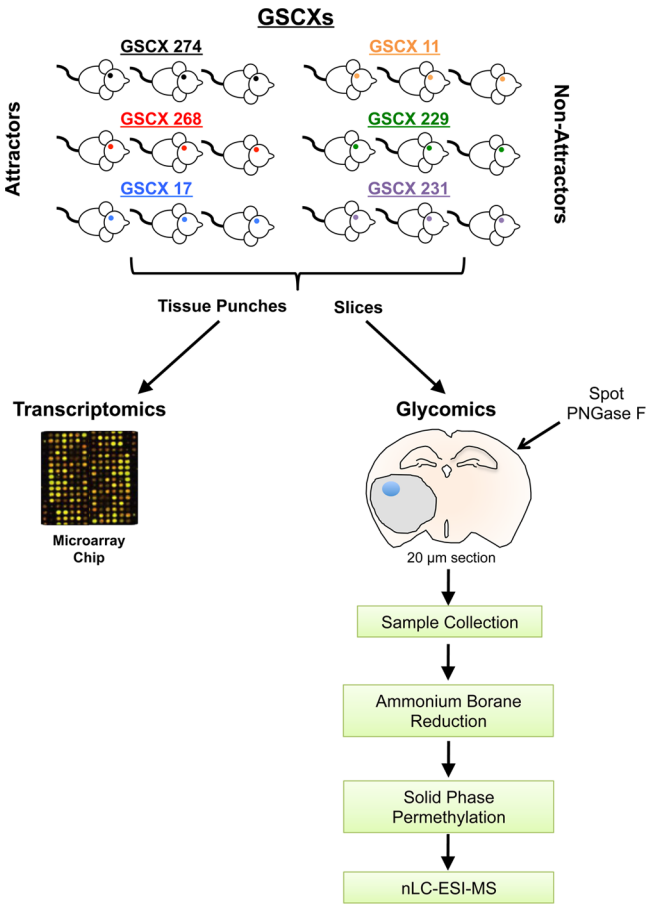


**Figure 1.** Workflow outlining tissue sample preparation for combined transcriptomics and glycomics. Tissue punches (left) from GSC xenografts (1.5 mm thick × 1.5 mm diameter) were taken for targeted transcriptomics (as described in Materials and Methods). Serial coronal sections from GSC xenografts at 20 $\mu$m (right) were made after the tissue punches were taken and thaw mounted on glass microscope slides. PNGase F (1 $\mu$L) was spotted on the tumors of each GSCX for *N*-glycan release overnight. Released *N*-glycans were collected, reduced, permethylated, and analyzed by nLC−ESI−MS.

## QUANTITATIVE GLYCOMICS OF ATTRACTOR RELATIVE TO NON-ATTRACTOR GSCXS

To corroborate the glycotranscriptomic findings and obtain tumor specific *N*-glycan information, we performed nLC−ESI−MS glycomic experiments from on-site PNGase F deglycosy-


DOI: 10.1021/acs.jproteome.5b00549
J. Proteome Res. 2015, 14, 3932−3939

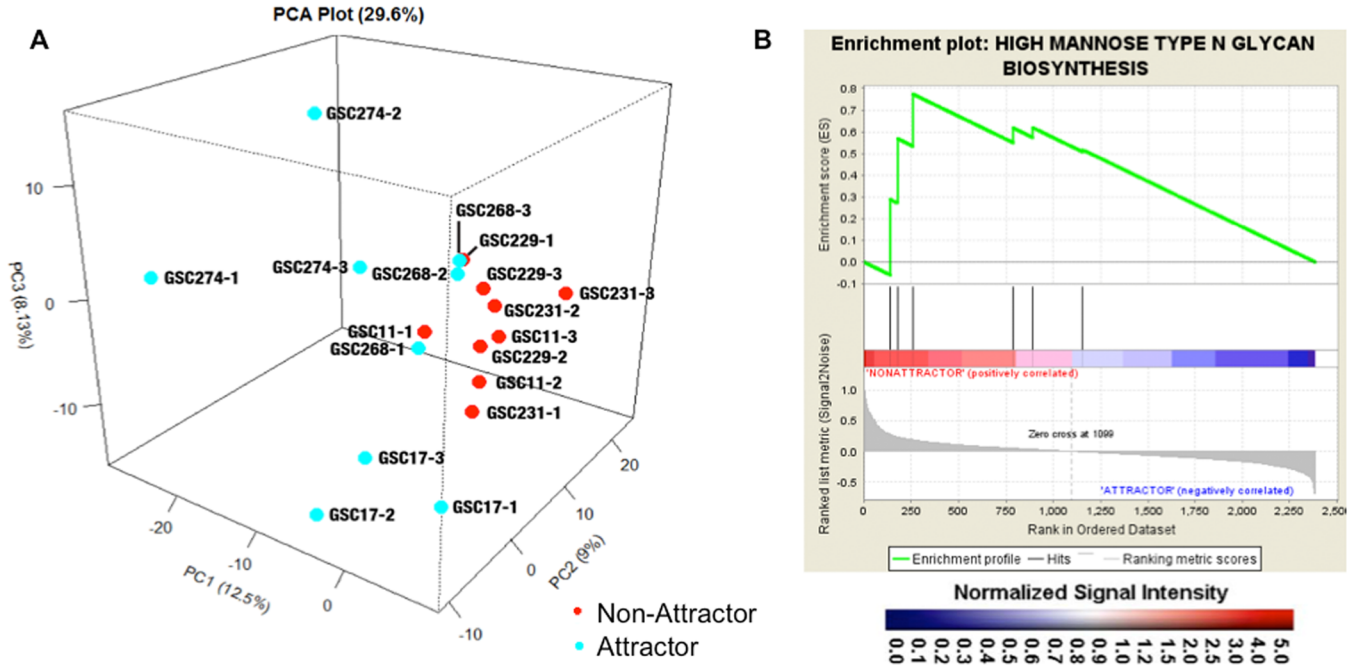


**Figure 2.** Targeted transcriptomic analysis. (A) Principal component analysis of all human glycogenes from targeted microarray. Attractors are in blue, and non-attractors are shown in red. GSC followed by a number designates the glioma stem cell line used for the xenograft, and the number following the hyphen indicates the biological replicate. (B) GSEA enrichment plots for statistically significant genes. The high mannose *N*-glycan type glycogene set enriched in the non-attractor phenotype is depicted. Black bars illustrate the position of the probe sets in the context of all of the glycoprobes on the array. The running enrichment score plotted as a function of the position of the ranked list of array probes is shown in green. The rank list metric shown in gray illustrates the correlation between the signal-to-noise values of all individually ranked genes according to the class labels (attractor vs non-attractor). The genes overrepresented on the leftmost side of the enrichment plots are those that correlate to differential expression in the non-attractor phenotype. Significantly enriched data sets are defined at $p < 0.05$ and false discovery rate (FDR) < 0.30.

lation of 20 $\mu$m coronal sections from the GSC xenografts. Of the detectible species passing our filters (Materials and Methods), we identified 18 glycan compositions, 9 of which were significantly differentially expressed between the two phenotypes (Figure 3). Consistent with our previous work,[21] there were more significant complex *N*-glycan compositions in the attractors compared to non-attractors. The high mannose glycans were significantly less abundant in the attractor phenotype in accordance with the GSEA biosynthesis pathway enrichment from the transcriptomic data (Figure 2). Further, the transcript *MAN1C1*, coding for the protein mannosyl-oligosaccharide 1,2-$\alpha$-mannosidase IC was decreased in attractors relative to non-attractors (Supplemental Table 1, Supporting Information). The *MAN1C1* enzyme produces $Man_8GlcNAc_2$, then $Man_6GlcNAc_2$, from $Man_9GlcNAc_2$, the nascent *N*-linked glycan emerging from the Golgi. Notably, $Man_6GlcNAc_2$ was one of the significant high mannose *N*-glycans found to be decreased in attractors compared to non-attractors.

Terminal mono- and disialylation of *N*-glycans ($GlcNAc_4Man_3Gal_2Sia_1$, $GlcNAc_4Man_4Gal_2Sia_2$, and $GlcNAc_4Man_4Gal_2Fuc_1Sia_1$) in the attractors was significantly decreased compared to the non-attractors; the presence of sialic acid on galactose could be either $\alpha$2−3 or $\alpha$2−6 linked.[5] This trend was consistent for those *N*-glycan compositions ($GlcNAc_4Man_3Gal_2Sia_1$, $GlcNAc_4Man_4Gal_2Sia_2$, and $GlcNAc_4Man_4Gal_2Fuc_1Sia_1$) that did not reach significance (Figure 3). The average peak areas of sialic acid-containing *N*-glycan species (Supplemental Figure 1, Supporting Information) support the overall trend of decreased sialic acid species in attractors compared to non-attractors ($p = 0.0001$). We note that the exception to this is *N*-glycan composition $GlcNAc_6Man_3Gal_4Fuc_2Sia_3$ (tetrantennary), which was increased in attractors and possesses three terminal sialic acids. Interestingly, $GlcNAc_6Man_3Gal_4Fuc_2Sia_3$ has a fucose on the antennae in addition to the core fucose, which must be $\alpha$1−6 linked, as PNGase F cannot cleave *N*-glycans containing core $\alpha$1−3 fucose. The fucose present on the *N*-glycan antenna is linked to the *N*-acetylglucosamine, which typically occurs as a $\alpha$1−3 or $\alpha$1−4 linkage. The transcript *FUT5* that codes for the enzyme $\alpha$-(1,3)-fucosyltransferase 5 was increased in attractors relative to non-attractors (Supplemental Table 1, Supporting Information). This enzyme is responsible for the placement of an $\alpha$1−4-linked fucose to *N*-acetyl-glucosamine (GlcNAc) and thus offers support for the *N*-glycan composition seen in $GlcNAc_6Man_3Gal_4Fuc_2Sia_3$.

In contrast, the *N*-glycan compositions increased in attractors compared to non-attractors are of the complex type, possessing either a terminal galactose or GlcNAc. Composition $GlcNAc_4Man_3Gal_2Fuc_1$ ($p = 0.02$) terminating in galactose was increased in attractors and compositions $GlcNAc_4Man_3Gal_1Fuc_1$ and $GlcNAc_7Man_3Gal_5$, while not significant, follow the same trend. Complex *N*-glycans $GlcNAc_4Man_3Fuc_1$ ($p = 0.0005$) and $GlcNAc_5Man_3Fuc_1$ ($p = 0.02$) are the two most abundant *N*-glycans in attractors and terminate with two or more GlcNAcs ($GlcNAc_4Man_3Fuc_1$ fold change = 4.4; $GlcNAc_5Man_3Fuc_1$ fold change = 3.7) in an *N*-acetyllactosamine (LacNAc) formation.[5] Composition $GlcNAc_3Man_3Fuc_1$ is an exception to this, however, ending with one GlcNAc monosaccharide at the reducing end, unlike compositions $GlcNAc_4Man_3Fuc_1$ and $GlcNAc_5Man_3Fuc_1$.


DOI: 10.1021/acs.jproteome.5b00549
J. Proteome Res. 2015, 14, 3932−3939

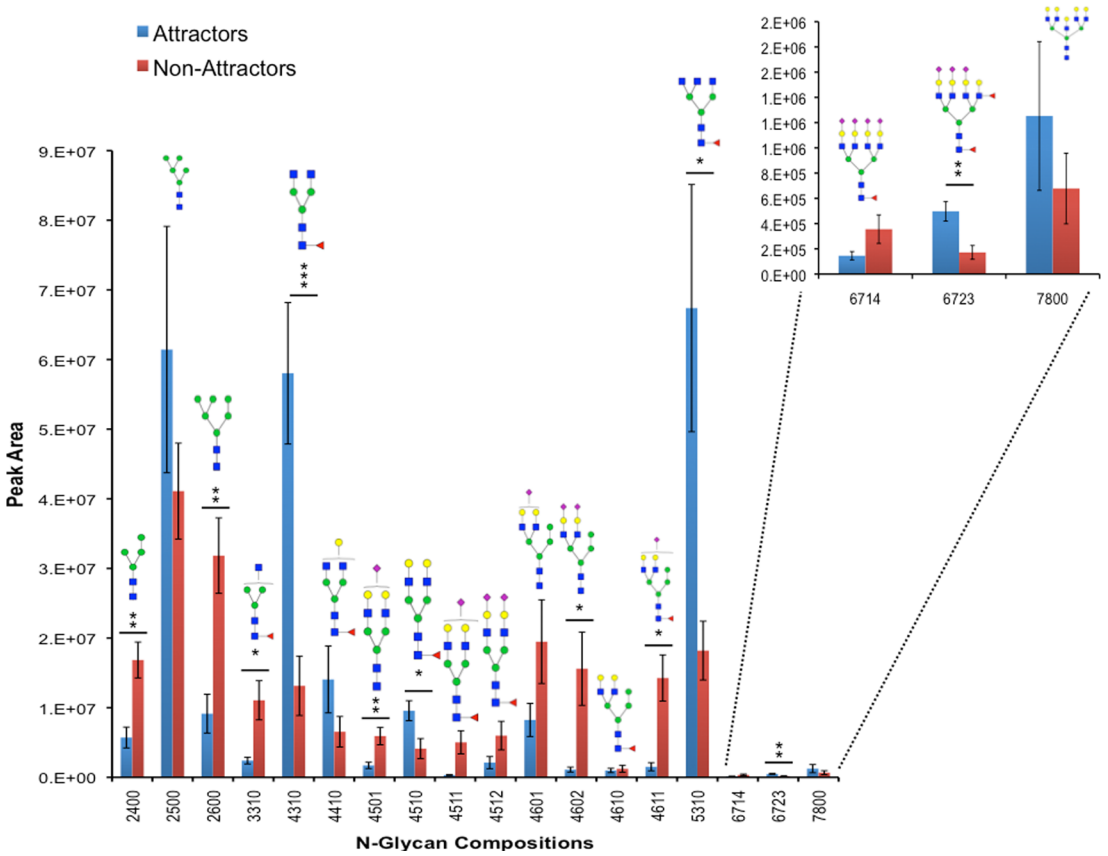


**Figure 3.** *N*-glycan Compositions in Attractors and Non-Attractors. Bar graphs of the permethylated *N*-glycan peak from attractor (blue) and non-attractor (red) GSCXs through on-tissue (tumor) digestion. The *y*-axis represents peak area, and the *x*-axis represents glycan composition (GlcNAc, Man, Gal, Fuc, NeuNAc). Symbols: GlcNAc, blue squares; Man, green circles; Gal, yellow circles; NeuNAc, magenta diamonds; and Fuc, red triangles. Values are mean ± SEM; $*p < 0.05$, $**p < 0.01$, and $***p < 0.001$ (Student's *t*-test).

## DISCUSSION

BM-hMSCs demonstrate significant promise as cell-based delivery vehicles for antiglioma therapeutics.[13,15−17,19,43,44] However, evidence suggests that in GSCXs, the "gold standard" of glioma models, these cells do not home or extravasate equally.[14] Given the importance of glycosylation in the extravasation process,[5,9,10] we examined the glycomic profile of attractors and non-attractors. The transcriptomic platform contains all human glycogenes, enabling analysis of all glycosylation pathways including, but not limited to, *N*- and *O*-linked glycosylation, gangliosides, and glycosaminoglycans. By utilizing this targeted transcriptomic approach, we were able to focus further glycomic studies on protein *N*-linked glycosylation in a data-driven approach for tumor-specific glycomic profiles. The value of this workflow is that the high-throughput targeted transcriptomic platform yields informative data about genes related to all types of glycosylation, which then serves to inform orthogonal glycomics experiments (Abstract Graphic and Figure 1).

The transcriptomic data revealed no significantly enriched glyco-synthetic or degradative pathways in attractors by use of GSEA analysis. This may be attributed to glycan heterogeneity in the attractor phenotype, which can clearly be seen in the PCA analysis (Figure 2A). However, high mannose biosynthesis was a significantly enriched *N*-linked glycosylation pathway in the non-attractor phenotype (Figure 2B), prompting us to examine the *N*-glycan profile of the GSCXs using the previously developed, highly efficient method for *N*-glycan profiling of tissue sections.[24] The utility of this approach is that information relevant to histopathology is obtained from small samples derived from xenografts.[24]

Orthogonal glycomic experiments confirmed elevated levels of high mannose *N*-glycans in the non-attractors (Figure 3), as predicted by GSEA analysis from the glycotranscriptomic data. High mannose *N*-glycans could be an indicator of an embryonic, undifferentiated phenotype.[45] Increased expression of high mannose type *N*-glycans has also been observed in colorectal cancer cell lines of varying malignancies[46−48] and in breast cancer cell lines and tissue.[49−51] The biological significance of this glycomic alteration in cancer is not clear, yet the presence of high (truncated) mannose indicates some level of incomplete *N*-linked glycosylation prossessing.[52] To what extent and whether or not the truncated high mannose is protein specific is unknown, as levels of terminal sialic acid (complex and hybrid) *N*-glycans, which represent uncompromised *N*-glycan processing, were increased in the non-attractors (Figure 3).

Sialic acids carry a strong negative charge and have dual biological functions.[5] They can act either as ligands for sialic acid binding proteins or they may serve to "mask" sites like galactose from galactose-binding receptors.[5,53] It has been observed that the increase in sialic acid content of tumor cells results in decreased attachment of the cell to the basement membrane via electrostatic repulsion, promoting metastasis.[5,53] Although GBM is confined within the cranium and does not metastasize, it is possible that via the same phenomenon, the


DOI: 10.1021/acs.jproteome.5b00549
J. Proteome Res. 2015, 14, 3932−3939

non-attractors repel BM-hMSCs, preventing extravasation and dispersion into the tumor parenchyma. Concomitantly, the sialic acid residues may be "masking" cell surface ligands that BM-hMSCs utilize for extravasation and dissemination throughout the tumor paraenchyma. For instance, sialic acid is known to inhibit galectin binding, which binds to either galactose or GlcNAc depending on the galectin isoform.[54,55] The structures increased in the attractors terminated in either GlcNAc or galactose, in contrast to their sialylated counterparts, which were increased in the non-attractors (Figure 3 and Supplemental Figure 1, Supporting Information). At present, only galectin-1 has been identified on the cell surface of BM-hMSCs.[56] The functional cell surface expression of other galectin isoforms on BM-hMSCs remains unresolved.

Interestingly, recent evidence suggests that sialic acids may scavenge free radicals, providing an antioxidant effect.[5,57−62] Sialic acids on glycosphingolipids have been reported to provide protection against ROS.[57,58] Free *N*-acetylneuraminic acid (Neu5Ac, sialic acid) in solution was able to reduce the concentration of organic peroxides, lipid hydroperoxides, and the arachidonic acid derivative HpETE as well as attenuate cytotoxicity in culture with these agents.[59,62] Pharmacologically, the hypersialylated analogue of human erythropoietin (r-HuEPO) was able to attenuate TNF-$\alpha$-induced ROS and activation of JNK and MSK1, kinases upstream of NFkB.[60] However, upon desialylation, r-HuEPO lost its ability to inhibit JNK and MSK1 and reduce TNF-$\alpha$-induced ROS.[60]

We have previously demonstrated that the pentose phosphate pathway (PPP) was downregulated in attractors relative to non-attractors.[21] Supporting this was the downregulation of glutathione S-transferase and superoxide dismutase in attractors relative to non-attractors and compromised fatty acid metabolism, which is heavily dependent on NADPH generated from the PPP.[21] These data suggest that reactive oxidative species (ROS), which incite pro-inflammatory reactions, in attractors would be more prevalent than in non-attractors. In fact, ROS species have been documented to decrease the sialic acid content of mammalian cell surface oligosaccharides,[63,64] which offers a possible explanation for the overall decreased levels of sialic acid-containing *N*-glycans in the attractors (Figure 3). The role of sialic acid-containing *N*-glycans as free radical scavengers[5,57−61] and its consistent upregulation in non-attractors in our glycomic study would presumably lead to lower levels of ROS and ROS-mediated inflammation in non-attractors. We note that our previous lipidomic study demonstrated DHA, an inflammatory-resolving lipid, to be increased in the tumor regions of non-attractors.[20] DHA is a fatty acid dependent upon NADPH generated by the PPP for its biosynthesis.[65] The PPP and the proteins directly and indirectly involved in DHA metabolism were upregulated in the non-attractor phenotype relative to the attractor phenotype, supporting decreased inflammation, including ROS-generated inflammation.[21] The increase in terminal sialic acid *N*-glycans in the non-attractor phenotype generates a new layer of complexity, adding new valuable information and supporting our previous work.[20,21]

Our study of the *N*-glycan profile of attractor and non-attractor GSCXs yielded highly informative *N*-glycan compositions from the tumor regions of glioma xenograft tissue. Because we applied the on-tissue PNGase F deglycosylation protocol,[24] we are confident that the *N*-glycan compositions we observed come from the cell surface in contrast to membrane fractionation, which invariably yields membrane contamination from the endoplasmic reticulum and Golgi apparatus.[45] However, we acknowledge that a limitation to this study is that the *N*-glycans and subsequent mass spectrometric measurements are derived from a thin slice of tissue, limiting the analytical depth of the tumor microenvironment and any *N*-glycan microheterogeneity associated with differential intratumoral microenvironments. Nonetheless, the results of this study motivate future investigations into the identity of proteins modified by *N*-glycans and their sites of attachment and linkage, along with mechanistic studies on their biological significance and functional relevance, including *N*-glycan expression by BM-hMSCs.

## ■ ASSOCIATED CONTENT

### Supporting Information

Number of sialic acid-containing *N*-glycan species in attractors relative to non-attractors and a complete list of significantly expressed transcripts. The Supporting Information is available free of charge on the ACS Publications website at DOI: 10.1021/acs.jproteome.5b00549.

## ■ AUTHOR INFORMATION


### Corresponding Authors

*Phone: +1 (806) 834 8246. Fax: +1 (806) 742 1289. E-mail: yehia.mechref@ttu.edu.

*Phone: +1 (409) 747 1840. Fax: +1 (409) 772 9648. E-mail: clnilsso@utmb.edu.


### Author Contributions

▽N.C.W. and S.Z. contributed equally to this work. N.C.W. conceived the study, performed experiments, data analysis and interpretation, and wrote the manuscript. S.Z. performed experiments, conducted data analysis and interpretation, and assisted in writing the manuscript. L.G.Z. performed glycan extractions, data acquisition, and data analysis. R.A.K. and J.R.M. contributed transcriptomics data analysis tools and provided helpful discussion. M.S. assisted in transcriptomics experiments and data analysis. P.M. assisted with glycan extractions. J.G. grew stem cell lines and performed all animal work. F.F.L., Y.M., and C.L.N. conceived the project, supervised the work, and critically revised the manuscript. All authors read and approved the final manuscript.

### Notes

The authors declare no competing financial interest.

## ■ ACKNOWLEDGMENTS


The authors gratefully acknowledge the financial support of the Cancer Prevention Research Institute of Texas (CPRIT) and The University of Texas Medical Branch to C.L.N., CPRIT (RP130624), NIH (GM-R01 GM112490-02) and Texas Tech University to Y.M., grants from the National Cancer Institute CA115729 and 1P50 CA127001, The Dr. Ralph and Marian Falk Medical Research Trust, Chicago IL to J.R.M., and The Broach Foundation for Brain Cancer Research, The Elias Family Fund, The National Brain Tumor Foundation, The Collaborative Ependymoma Research network (CERN), The Gene Pennebaker Brain Cancer Fund, the Sorenson Foundation, and the Brian McCulloch Fund to F.F.L.




DOI: 10.1021/acs.jproteome.5b00549
J. Proteome Res. 2015, 14, 3932−3939

## REFERENCES


(1) Apweiler, R.; Hermjakob, H.; Sharon, N. On the frequency of protein glycosylation, as deduced from analysis of the SWISS-PROT database. *Biochim. Biophys. Acta, Gen. Subj.* **1999**, *1473*, 4−8.

(2) *Genomics and proteomics for clinical discovery and development*. Marko-Varga, G., Ed.; Springer: New York, 2014.

(3) Dwek, R. A. Glycobiology: Toward Understanding the Function of Sugars. *Chem. Rev.* **1996**, *96*, 683−720.

(4) Varki, A. Biological roles of oligosaccharides: all of the theories are correct. *Glycobiology* **1993**, *3*, 97−130.

(5) Varki, A. *Essentials of glycobiology*, 2nd ed.; Cold Spring Harbor Laboratory Press: Cold Spring Harbor, N.Y., 2009; Vol. *xxix*, p 784.

(6) Ohtsubo, K.; Marth, J. D. Glycosylation in cellular mechanisms of health and disease. *Cell* **2006**, *126*, 855−67.

(7) Baum, L. G.; Garner, O. B.; Schaefer, K.; Lee, B. Microbe-Host Interactions are Positively and Negatively Regulated by Galectin-Glycan Interactions. *Front. Immunol.* **2014**, *5*, 284.

(8) Ferluga, S.; Hantgan, R.; Goldgur, Y.; Himanen, J. P.; Nikolov, D. B.; Debinski, W. Biological and structural characterization of glycosylation on ephrin-A1, a preferred ligand for EphA2 receptor tyrosine kinase. *J. Biol. Chem.* **2013**, *288*, 18448−57.

(9) Scott, D. W.; Patel, R. P. Endothelial heterogeneity and adhesion molecules N-glycosylation: implications in leukocyte trafficking in inflammation. *Glycobiology* **2013**, *23*, 622−33.

(10) Wright, R. D.; Cooper, D. Glycobiology of leukocyte trafficking in inflammation. *Glycobiology* **2014**, *24*, 1242−51.

(11) Block, H.; Ley, K.; Zarbock, A. Severe impairment of leukocyte recruitment in ppGalNAcT-1-deficient mice. *J. Immunol.* **2012**, *188*, 5674−81.

(12) Frommhold, D.; Ludwig, A.; Bixel, M. G.; Zarbock, A.; Babushkina, I.; Weissinger, M.; Cauwenberghs, S.; Ellies, L. G.; Marth, J. D.; Beck-Sickinger, A. G.; Sixt, M.; Lange-Sperandio, B.; Zernecke, A.; Brandt, E.; Weber, C.; Vestweber, D.; Ley, K.; Sperandio, M. Sialyltransferase ST3Gal-IV controls CXCR2-mediated firm leukocyte arrest during inflammation. *J. Exp. Med.* **2008**, *205*, 1435−46.

(13) Kosztowski, T.; Zaidi, H. A.; Quiñones-Hinojosa, A. Applications of neural and mesenchymal stem cells in the treatment of gliomas. *Expert Rev. Anticancer Ther.* **2009**, *9*, 597−612.

(14) Shinojima, N.; Hossain, A.; Takezaki, T.; Fueyo, J.; Gumin, J.; Gao, F.; Nwajei, F.; Marini, F. C.; Andreeff, M.; Kuratsu, J.; Lang, F. F. TGF-$\beta$ mediates homing of bone marrow-derived human mesenchymal stem cells to glioma stem cells. *Cancer Res.* **2013**, *73*, 2333−44.

(15) Yong, R. L.; Shinojima, N.; Fueyo, J.; Gumin, J.; Vecil, G. G.; Marini, F. C.; Bogler, O.; Andreeff, M.; Lang, F. F. Human bone marrow-derived mesenchymal stem cells for intravascular delivery of oncolytic adenovirus Delta24-RGD to human gliomas. *Cancer Res.* **2009**, *69*, 8932−40.

(16) Nakamizo, A.; Marini, F.; Amano, T.; Khan, A.; Studeny, M.; Gumin, J.; Chen, J.; Hentschel, S.; Vecil, G.; Dembinski, J.; Andreeff, M.; Lang, F. F. Human bone marrow-derived mesenchymal stem cells in the treatment of gliomas. *Cancer Res.* **2005**, *65*, 3307−18.

(17) Nakamura, K.; Ito, Y.; Kawano, Y.; Kurozumi, K.; Kobune, M.; Tsuda, H.; Bizen, A.; Honmou, O.; Niitsu, Y.; Hamada, H. Antitumor effect of genetically engineered mesenchymal stem cells in a rat glioma model. *Gene Ther.* **2004**, *11*, 1155−64.

(18) Studeny, M.; Marini, F. C.; Champlin, R. E.; Zompetta, C.; Fidler, I. J.; Andreeff, M. Bone marrow-derived mesenchymal stem cells as vehicles for interferon-beta delivery into tumors. *Cancer Res.* **2002**, *62*, 3603−3608.

(19) Studeny, M.; Marini, F. C.; Dembinski, J. L.; Zompetta, C.; Cabreira-Hansen, M.; Bekele, B. N.; Champlin, R. E.; Andreeff, M. Mesenchymal stem cells: potential precursors for tumor stroma and targeted-delivery vehicles for anticancer agents. *J. Natl. Cancer Inst* **2004**, *96*, 1593−603.

(20) Wildburger, N. C.; Wood, P. L.; Gumin, J.; Lichti, C. F.; Emmett, M. R.; Lang, F. F.; Nilsson, C. L. ESI-MS/MS and MALDI-IMS Localization Reveal Alterations in Phosphatidic Acid, Diacylglycerol, and DHA in Glioma Stem Cell Xenografts. *J. Proteome Res.* **2015**, *14*, 2511−9.

(21) Wildburger, N. C.; Lichti, C. F.; LeDuc, R. D.; Gumin, J.; Schmidt, M.; Kroes, R. A.; Moskal, J. R.; Lang, F. F.; Nilsson, C. L. Quantitative Proteomics Reveals Metabolic Differences in Glioma Stem Cell Xenografts and Stromal Cells. *EuPa Open Proteomics* **2015**, DOI: 10.1016/j.euprot.2015.06.006.

(22) Kroes, R. A.; He, H.; Emmett, M. R.; Nilsson, C. L.; Leach, F. E.; Amster, I. J.; Marshall, A. G.; Moskal, J. R. Overexpression of ST6GalNAcV, a ganglioside-specific alpha2,6-sialyltransferase, inhibits glioma growth in vivo. *Proc. Natl. Acad. Sci. U. S. A.* **2010**, *107*, 12646−51.

(23) He, H.; Nilsson, C. L.; Emmett, M. R.; Marshall, A. G.; Kroes, R. A.; Moskal, J. R.; Ji, Y.; Colman, H.; Priebe, W.; Lang, F. F.; Conrad, C. A. Glycomic and transcriptomic response of GSC11 glioblastoma stem cells to STAT3 phosphorylation inhibition and serum-induced differentiation. *J. Proteome Res.* **2010**, *9*, 2098−108.

(24) Hu, Y.; Zhou, S.; Khalil, S. I.; Renteria, C. L.; Mechref, Y. Glycomic profiling of tissue sections by LC-MS. *Anal. Chem.* **2013**, *85*, 4074−9.

(25) Singh, S. K.; Clarke, I. D.; Terasaki, M.; Bonn, V. E.; Hawkins, C.; Squire, J.; Dirks, P. B. Identification of a cancer stem cell in human brain tumors. *Cancer Res.* **2003**, *63*, 5821−5828.

(26) Singh, S. K.; Hawkins, C.; Clarke, I. D.; Squire, J. A.; Bayani, J.; Hide, T.; Henkelman, R. M.; Cusimano, M. D.; Dirks, P. B. Identification of human brain tumour initiating cells. *Nature* **2004**, *432*, 396−401.

(27) Lal, S.; Lacroix, M.; Tofilon, P.; Fuller, G. N.; Sawaya, R.; Lang, F. F. An implantable guide-screw system for brain tumor studies in small animals. *J. Neurosurg.* **2000**, *92*, 326−33.

(28) Shavkunov, A. S.; Wildburger, N. C.; Nenov, M. N.; James, T. F.; Buzhdygan, T. P.; Panova-Elektronova, N. I.; Green, T. A.; Veselenak, R. L.; Bourne, N.; Laezza, F. The fibroblast growth factor 14·voltage-gated sodium channel complex is a new target of glycogen synthase kinase 3 (GSK3). *J. Biol. Chem.* **2013**, *288*, 19370−85.

(29) Kroes, R. A.; Panksepp, J.; Burgdorf, J.; Otto, N. J.; Moskal, J. R. Modeling depression: social dominance-submission gene expression patterns in rat neocortex. *Neuroscience* **2006**, *137*, 37−49.

(30) Kroes, R. A.; Dawson, G.; Moskal, J. R. Focused microarray analysis of glyco-gene expression in human glioblastomas. *J. Neurochem.* **2007**, *103* (Suppl 1), 14−24.

(31) Nilsson, C. L.; Berven, F.; Selheim, F.; Liu, H.; Moskal, J. R.; Kroes, R. A.; Sulman, E. P.; Conrad, C. A.; Lang, F. F.; Andrén, P. E.; Nilsson, A.; Carlsohn, E.; Lilja, H.; Malm, J.; Fenyö, D.; Subramaniyam, D.; Wang, X.; Gonzales-Gonzales, M.; Dasilva, N.; Diez, P.; Fuentes, M.; Végvári, Á.; Sjödin, K.; Welinder, C.; Laurell, T.; Fehniger, T. E.; Lindberg, H.; Rezeli, M.; Edula, G.; Hober, S.; Marko-Varga, G. Chromosome 19 annotations with disease speciation: a first report from the Global Research Consortium. *J. Proteome Res.* **2013**, *12*, 135−50.

(32) Churchill, G. A. Fundamentals of experimental design for cDNA microarrays. *Nat. Genet.* **2002**, *32* (Suppl), 490−5.

(33) Tusher, V. G.; Tibshirani, R.; Chu, G. Significance analysis of microarrays applied to the ionizing radiation response. *Proc. Natl. Acad. Sci. U. S. A.* **2001**, *98*, 5116−21.

(34) Subramanian, A.; Tamayo, P.; Mootha, V. K.; Mukherjee, S.; Ebert, B. L.; Gillette, M. A.; Paulovich, A.; Pomeroy, S. L.; Golub, T. R.; Lander, E. S.; Mesirov, J. P. Gene set enrichment analysis: a knowledge-based approach for interpreting genome-wide expression profiles. *Proc. Natl. Acad. Sci. U. S. A.* **2005**, *102*, 15545−50.

(35) Mootha, V. K.; Lindgren, C. M.; Eriksson, K. F.; Subramanian, A.; Sihag, S.; Lehar, J.; Puigserver, P.; Carlsson, E.; Ridderstråle, M.; Laurila, E.; Houstis, N.; Daly, M. J.; Patterson, N.; Mesirov, J. P.; Golub, T. R.; Tamayo, P.; Spiegelman, B.; Lander, E. S.; Hirschhorn, J. N.; Altshuler, D.; Groop, L. C. PGC-1alpha-responsive genes involved in oxidative phosphorylation are coordinately downregulated in human diabetes. *Nat. Genet.* **2003**, *34*, 267−73.

(36) Crosson, L. A.; Kroes, R. A.; Moskal, J. R.; Linsenmeier, R. A. Gene expression patterns in hypoxic and post-hypoxic adult rat retina with special reference to the NMDA receptor and its interactome. *Mol. Vision* **2009**, *15*, 296−311.




DOI: 10.1021/acs.jproteome.5b00549
*J. Proteome Res.* 2015, 14, 3932−3939

(37) Desantos-Garcia, J. L.; Khalil, S. I.; Hussein, A.; Hu, Y.; Mechref, Y. Enhanced sensitivity of LC-MS analysis of permethylated N-glycans through online purification. *Electrophoresis* **2011**, *32*, 3516−25.
(38) Hu, Y.; Mechref, Y. Comparing MALDI-MS, RP-LC-MALDI-MS and RP-LC-ESI-MS glycomic profiles of permethylated N-glycans derived from model glycoproteins and human blood serum. *Electrophoresis* **2012**, *33*, 1768−77.
(39) Hu, Y.; Desantos-Garcia, J. L.; Mechref, Y. Comparative glycomic profiling of isotopically permethylated N-glycans by liquid chromatography/electrospray ionization mass spectrometry. *Rapid Commun. Mass Spectrom.* **2013**, *27*, 865−77.
(40) Tsai, T. H.; Wang, M.; Di Poto, C.; Hu, Y.; Zhou, S.; Zhao, Y.; Varghese, R. S.; Luo, Y.; Tadesse, M. G.; Ziada, D. H.; Desai, C. S.; Shetty, K.; Mechref, Y.; Ressom, H. W. LC-MS profiling of N-Glycans derived from human serum samples for biomarker discovery in hepatocellular carcinoma. *J. Proteome Res.* **2014**, *13*, 4859−68.
(41) Hu, Y.; Zhou, S.; Yu, C. Y.; Tang, H.; Mechref, Y. Automated annotation and quantitation of glycans by liquid chromatography/electrospray ionization mass spectrometric analysis using the Multi-Glycan-ESI computational tool. *Rapid Commun. Mass Spectrom.* **2015**, *29*, 135−42.
(42) Yu, C. Y.; Mayampurath, A.; Hu, Y.; Zhou, S.; Mechref, Y.; Tang, H. Automated annotation and quantification of glycans using liquid chromatography-mass spectrometry. *Bioinformatics* **2013**, *29*, 1706−7.
(43) Miletic, H.; Fischer, Y.; Litwak, S.; Giroglou, T.; Waerzeggers, Y.; Winkeler, A.; Li, H.; Himmelreich, U.; Lange, C.; Stenzel, W.; Deckert, M.; Neumann, H.; Jacobs, A. H.; von Laer, D. Bystander killing of malignant glioma by bone marrow-derived tumor-infiltrating progenitor cells expressing a suicide gene. *Mol. Ther.* **2007**, *15*, 1373−81.
(44) Doucette, T.; Rao, G.; Yang, Y.; Gumin, J.; Shinojima, N.; Bekele, B. N.; Qiao, W.; Zhang, W.; Lang, F. F. Mesenchymal stem cells display tumor-specific tropism in an RCAS/Ntv-a glioma model. *Neoplasia* **2011**, *13*, 716−25.
(45) An, H. J.; Gip, P.; Kim, J.; Wu, S.; Park, K. W.; McVaugh, C. T.; Schaffer, D. V.; Bertozzi, C. R.; Lebrilla, C. B. Extensive determination of glycan heterogeneity reveals an unusual abundance of high mannose glycans in enriched plasma membranes of human embryonic stem cells. *Mol. Cell. Proteomics* **2012**, *11*, M111.010660.
(46) Sethi, M. K.; Thaysen-Andersen, M.; Smith, J. T.; Baker, M. S.; Packer, N. H.; Hancock, W. S.; Fanayan, S. Comparative N-glycan profiling of colorectal cancer cell lines reveals unique bisecting GlcNAc and α-2,3-linked sialic acid determinants are associated with membrane proteins of the more metastatic/aggressive cell lines. *J. Proteome Res.* **2014**, *13*, 277−88.
(47) Balog, C. I.; Stavenhagen, K.; Fung, W. L.; Koeleman, C. A.; McDonnell, L. A.; Verhoeven, A.; Mesker, W. E.; Tollenaar, R. A.; Deelder, A. M.; Wuhrer, M. N-glycosylation of colorectal cancer tissues: a liquid chromatography and mass spectrometry-based investigation. *Mol. Cell. Proteomics* **2012**, *11*, 571−85.
(48) Holst, S.; Wuhrer, M.; Rombouts, Y. Glycosylation characteristics of colorectal cancer. *Adv. Cancer Res.* **2015**, *126*, 203−256.
(49) Hua, S.; Saunders, M.; Dimapasoc, L. M.; Jeong, S. H.; Kim, B. J.; Kim, S.; So, M.; Lee, K. S.; Kim, J. H.; Lam, K. S.; Lebrilla, C. B.; An, H. J. Differentiation of cancer cell origin and molecular subtype by plasma membrane N-glycan profiling. *J. Proteome Res.* **2014**, *13*, 961−8.
(50) Liu, X.; Nie, H.; Zhang, Y.; Yao, Y.; Maitikabili, A.; Qu, Y.; Shi, S.; Chen, C.; Li, Y. Cell surface-specific N-glycan profiling in breast cancer. *PLoS One* **2013**, *8*, e72704.
(51) de Leoz, M. L.; Young, L. J.; An, H. J.; Kronewitter, S. R.; Kim, J.; Miyamoto, S.; Borowsky, A. D.; Chew, H. K.; Lebrilla, C. B. High-mannose glycans are elevated during breast cancer progression. *Mol. Cell. Proteomics* **2011**, *10*, M110.002717.
(52) Hakomori, S. Aberrant glycosylation in cancer cell membranes as focused on glycolipids: overview and perspectives. *Cancer Res.* **1985**, *45*, 2405−2414.
(53) Schultz, M. J.; Swindall, A. F.; Bellis, S. L. Regulation of the metastatic cell phenotype by sialylated glycans. *Cancer Metastasis Rev.* **2012**, *31*, 501−18.
(54) Hirabayashi, J.; Hashidate, T.; Arata, Y.; Nishi, N.; Nakamura, T.; Hirashima, M.; Urashima, T.; Oka, T.; Futai, M.; Muller, W. E.; Yagi, F.; Kasai, K. Oligosaccharide specificity of galectins: a search by frontal affinity chromatography. *Biochim. Biophys. Acta, Gen. Subj.* **2002**, *1572*, 232−254.
(55) Zhuo, Y.; Bellis, S. L. Emerging role of alpha2,6-sialic acid as a negative regulator of galectin binding and function. *J. Biol. Chem.* **2011**, *286*, 5935−41.
(56) Siegel, G.; Kluba, T.; Hermanutz-Klein, U.; Bieback, K.; Northoff, H.; Schäfer, R. Phenotype, donor age and gender affect function of human bone marrow-derived mesenchymal stromal cells. *BMC Med.* **2013**, *11*, 146.
(57) Gavella, M.; Garaj-Vrhovac, V.; Lipovac, V.; Antica, M.; Gajski, G.; Car, N. Ganglioside GT1b protects human spermatozoa from hydrogen peroxide-induced DNA and membrane damage. *Int. J. Androl.* **2010**, *33*, 536−44.
(58) Gavella, M.; Lipovac, V. Protective effects of exogenous gangliosides on ROS-induced changes in human spermatozoa. *Asian J. Androl.* **2013**, *15*, 375−81.
(59) Iijima, R.; Ichikawa, T.; Yamazaki, M. Sialic acid attenuates the cytotoxicity of the lipid hydroperoxides HpODE and HpETE. *Carbohydr. Res.* **2009**, *344*, 933−5.
(60) Yang, W. S.; Chang, J. W.; Han, N. J.; Park, S. K. Darbepoetin alfa suppresses tumor necrosis factor-α-induced endothelin-1 production through antioxidant action in human aortic endothelial cells: role of sialic acid residues. *Free Radical Biol. Med.* **2011**, *50*, 1242−51.
(61) Ogasawara, Y.; Namai, T.; Yoshino, F.; Lee, M. C.; Ishii, K. Sialic acid is an essential moiety of mucin as a hydroxyl radical scavenger. *FEBS Lett.* **2007**, *581*, 2473−7.
(62) Iijima, R.; Takahashi, H.; Namme, R.; Ikegami, S.; Yamazaki, M. Novel biological function of sialic acid (N-acetylneuraminic acid) as a hydrogen peroxide scavenger. *FEBS Lett.* **2004**, *561*, 163−6.
(63) Eguchi, H.; Ikeda, Y.; Ookawara, T.; Koyota, S.; Fujiwara, N.; Honke, K.; Wang, P. G.; Taniguchi, N.; Suzuki, K. Modification of oligosaccharides by reactive oxygen species decreases sialyl lewis x-mediated cell adhesion. *Glycobiology* **2005**, *15*, 1094−1101.
(64) Yasuda, J.; Eguchi, H.; Fujiwara, N.; Ookawara, T.; Kojima, S.; Yamaguchi, Y.; Nishimura, M.; Fujimoto, J.; Suzuki, K. Reactive oxygen species modify oligosaccharides of glycoproteins in vivo: a study of a spontaneous acute hepatitis model rat (LEC rat). *Biochem. Biophys. Res. Commun.* **2006**, *342*, 127−34.
(65) Kang, S. W.; Lee, S.; Lee, E. K. ROS and energy metabolism in cancer cells: alliance for fast growth. *Arch. Pharmacal Res.* **2015**, *38*, 338−45.


DOI: 10.1021/acs.jproteome.5b00549
*J. Proteome Res.* 2015, 14, 3932−3939